Monoclinic to tetragonal semireconstructive phase transition of zirconia

D. Simeone
Laboratoire de Métallurgie Structurale, CEA/Saclay F-91191 Gif sur Yvette, France

G. Baldinozzi
Laboratoire de Structures, Propriétés et Modélisation des Solides, UMR CNRS 8580 Ecole Centrale Paris, F-92295 Châtenay Malabry, France

D. Gosset and M. Dutheil
Laboratoire de Métallurgie Structurale, CEA/Saclay F-91191 Gif sur Yvette, France

A. Bulou
Laboratoire de Physique de l'Etat Condensé, UMR 6087, F-72085 le Mans Cedex 09, France

T. Hansen
ILL BP 43, F-38042 Grenoble cedex, France

(Received 26 June 2002; revised manuscript received 27 September 2002; published 28 February 2003)

Accurate data, obtained by neutron diffraction, have been used to monitor the first-order reconstructive monoclinic↔tetragonal phase transition as a function of the temperature both during heating and cooling. Data analysis supports an orientational relationship $[010]_m \| [001]_t$ and $(100)_m \| (110)_t$ between the tetragonal and the monoclinic phases. The analysis of the oxygen atoms evolution in the tetragonal phase supports a displacive mechanism for the monoclinic↔tetragonal phase transition. Based on these data, a microscopic model is proposed explaining the unusual behavior of zirconia.

DOI: 10.1103/PhysRevB.67.064111 PACS number(s): 61.12.Ld, 64.60.Fr

I. INTRODUCTION

Zirconia is an interesting technological material because of its outstanding mechanical and electrical properties.[1] In particular, the possibility to accept selective substitutions makes zirconia a good host for nuclear wastes. Therefore assessing the stability of the structure is of paramount importance to match the severe nuclear standards. Unfortunately, under irradiation,[2] the room-temperature monoclinic phase undergoes a first-order phase transition characterized by an important volume variation. The onset of large strain fields in the material is responsible for the consequent integrity loss and migration of nuclear wastes out of the matrix. The same monoclinic to tetragonal phase transition is observed in undoped zirconia at about 1400 K. Understanding the mechanism of this phase transition in pure ZrO_2 at a microscopic level can help to improve the stability of this material.

Zirconium and oxygen atoms sit in a fluorite structure ($Fm\bar{3}m$ space group) below the melting temperature (2973 K). Zirconia undergoes two successive phase transitions on cooling. The former transition occurs at about 2573 K and it is second order or weakly first order.[3,4] The cubic structure becomes tetragonal ($P4_2/nmc$) and it is characterized in particular by the onset of a shear strain along the fourfold axis; the coordination polyhedron for Zr in the ideal fluorite structure (ZrO_8 unit) is only sligthly modified. On the other hand, the second phase transition, occurring at about 1330 K on cooling and at about 1500 K on heating, involves important variations of unit-cell parameters. This transition, associated with an important volume change, is strongly first order. In the monoclinic phase, stable at room temperature and ambient pressure, the Zr polyhedron is strongly distorted and two independent O atoms are necessary to describe the structure: the O(1) atoms define a triangular pyramid with the Zr cation setting at the apex; the O(2) atoms form, with the same Zr atom, a square pyramid corresponding to one-half the normal ZrO_8 unit of the ideal fluorite structure.[5] Therefore this transition can be considered as semireconstructive. Nevertheless, it is nowadays commonly accepted that this first-order phase transition has a displacive character[6] and some authors propose to describe this transition within the soft-mode formalism.[7–9] As a matter of fact, lattice dynamic calculations based on empirical Born-Mayer short-range potentials[10,11] predict the existence of soft phonons in the tetragonal phase.[12,13] Phonons frequencies obtained from these calculations disagree with the *abinitio* calculation results.[14,15] Up to now, the structural data (atomic positions, anisotropic thermal displacements, etc.) extracted from diffraction measurements versus temperature are not accurate enough to check this mechanism.[16,17] The aim of this work is to obtain improved structural data near the transition temperature in order to estabilish a microscopic mechanism of this phase transformation. To this purpose, we have collected several high-resolution neutron-diffraction patterns at different temperatures above and below the tetragonal to monoclinic transition and analyzed these results within the Rietveld method to extract the behavior of the structural parameters and to describe their evolution in the framework of the Landau theory of the second-order phase transition.

II. EXPERIMENT

The sample was a high-purity (about 99.92%) commercial ZrO_2 powder (Alfa-Aesar Co.) with an average grain size

smaller than 10 μm. The experiment was carried out at the high-resolution and high flux neutron powder diffractometer D20 at ILL using a wavelength of 1.28 Å obtained from a vertically focusing graphite monochromator. The powder was put in an open Pt cylinder placed at the common focus of two ellipsoidal mirrors and heated by two halogen lamps. Data were collected on heating and on cooling between room temperature and 1600 K and analyzed by a multiphase Rietveld program (XND).[18] The few diffraction peaks of the Pt sample holder were handled as a parasitic phase since either they do not overlap or they can be easily distinguished and deconvoluted from the zirconia ones. Atomic positions and anisotropic thermal displacement parameters for all atoms in zirconia were refined at all temperatures in the tetragonal and monoclinc phases. The occupancies of zirconium and oxygen atoms were checked throughout the refinements and they do not change from their nominal values, either on heating or on cooling, as previously observed.[16,17] Since neutron-scattering lengths for O (b_O=5.80 fm) and Zr atoms (b_{Zr}=7.16 fm) are of the same order, the accuracies on the structural parameters for all atoms are better than those obtained from x-ray diffraction.

III. RESULTS

The diffraction pattens in the tetragonal and in the monoclinic phases are consistent with the $P2_1/c$ and $P4_2/nmc$ space groups, respectively. Structural refinements give good reliability factors, $R_{Bragg} \leqslant 3\%$, in the single phase region, and about 5% in the two phase range. Figure 1 displays the temperature evolution of the volumic fraction of the tetragonal phase during the transition. The width of the hysteresis extends over 170 K (1325–1495 K) in good agreement with previous observations.[5] The scale factors variations of the two phases are too small to suggest a significant disorder or an additional short-range-order modulation. Further careful examination of the integrated intensities of monoclinic, $(111)_m$, $(1\bar{1}1)_m$, $(002)_m$, $(020)_m$, and tetragonal, $(101)_t$, $(110)_t$, $(002)_t$, peaks does not indicate any abnormal intensity variation versus temperature such as those previously reported by x-ray studies.[6]

The analysis of the symmetry elements associated with both phases clearly suggests a correspondence between the monoclinic axis and the fourfold axis in the tetragonal phase. Following the work of Wolten,[19] we have choosen the $[010]_m \| [001]_t$ and $(100)_m \| (110)_t$ orientational relations between the two phases since $a_m \sin\beta$ is close to $\sqrt{2}a_t$ (Fig. 2). The evolution of these unit-cell parameters in both phases is linear. The values of the thermal-expansion coefficients in the two phases, extracted from this refinement, are summarized and compared to previous experiments[6,20] in Table I.

On the other hand, an important deviation from linearity is observed for a_t and c_t below 1400 K on heating and below 1200 K on cooling (Fig. 2). This remarkable behavior, already observed by some authors,[17] occurs for low volumic fractions of the tetragonal phase (cf. Fig. 1) and could be interpreted as the signature of an important macroscopic strain on the tetragonal phase induced by the appearance of the monoclinc phase. The volume difference between the two

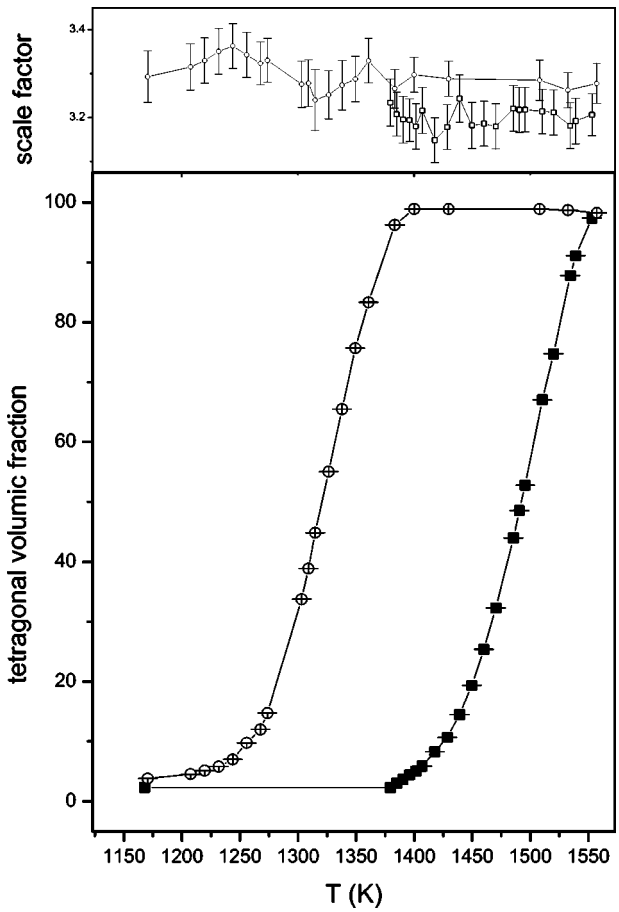

FIG. 1. Bottom panel: evolution of the tetragonal volumic fraction of ZrO_2 on heating (squares) and on cooling (open dots) as a function of temperature. Top panel: the evolution of the scale factor on heating and on cooling does not exhibit any particular variation.

phases is responsible for this macroscopic strain and it may explain the important hysteresis range of this transition. Figure 3 presents the evolution of the $(\beta-\pi/2)$ angle associated with the monoclinic distortion as a function of (T_c-T) where T_c is the critical temperature associated with the transition.[21] This distortion presents a linear dependence between the transition temperature (1500 K) and 1200 K. Below this temperature it follows a square-root law. This change of the behavior of the monoclinic distortion suggests that a crossover mechanism occurs and a microscopic model for this phase transition should actually reproduce this feature.

To follow the structural evolution of the atomic displacements in the tetragonal phase, the oxygen position z_t(O) along the fourfold axis and anisotropic mean-square displacements of both atoms (u^{ij}) were refined. The correlation between z_t(O) and (u^{ij}) for the oxygen atoms is not significant. At high temperature, no thermal evolution of the oxygen position along the fourfold axis is observed. This suggests that the mechanism responsible for the transition from the cubic to the tetragonal phase is already completed. On the other hand, the amplitudes of some components of the anisotropic thermal displacement parameters of O (u^{33}) and Zr (u^{11}) in the tetragonal phase significantly increase on

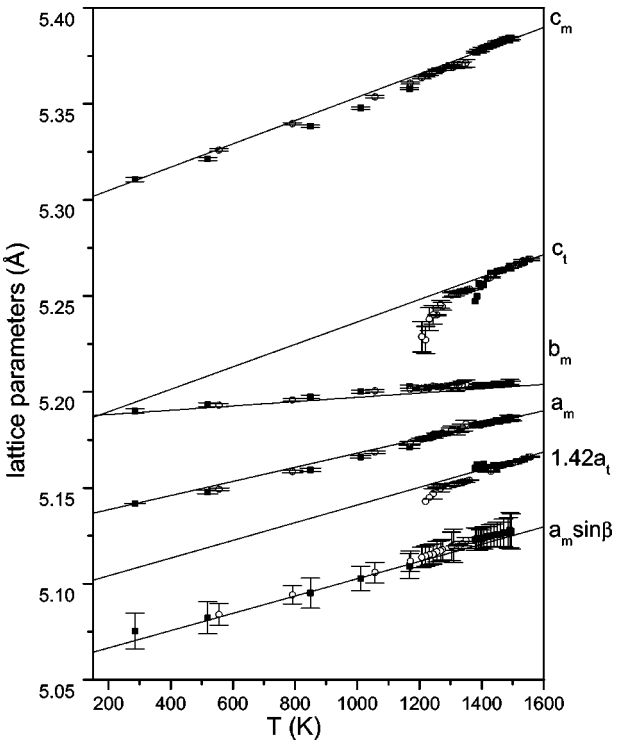

FIG. 2. Evolution of the unit-cell parameters (a,b,c) of the monoclinic (subscript m) and tetragonal (subscript t) phases during heating (squares) and cooling (open dots).

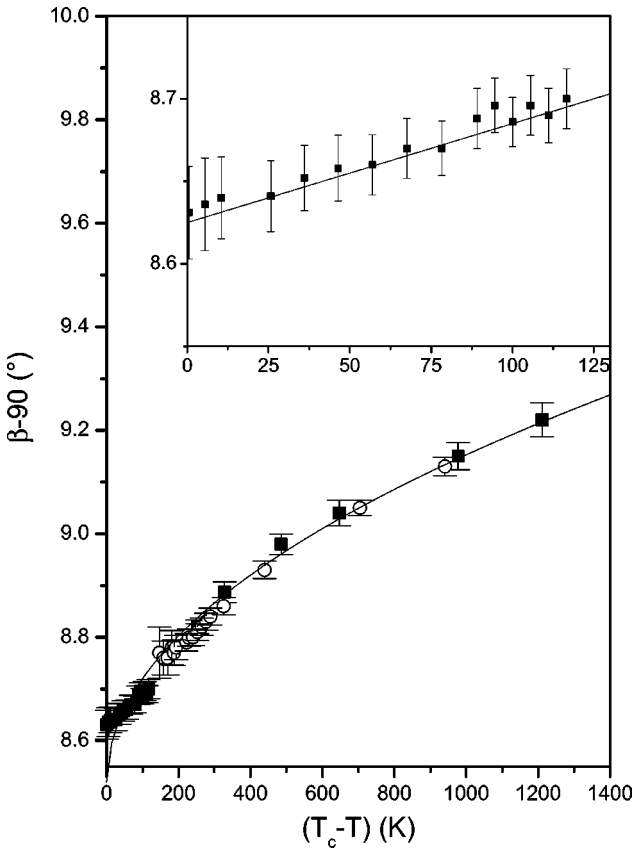

FIG. 3. Evolution of the monoclinic $\beta-\pi/2$ distortion angle as a function of the temperature. The evolution on heating (squares) and on cooling (open dots) of the distortion is plotted as a function of (T_c-T) with T_c equal to 1500 K. The data fit (solid line) is linear for small values of (T_c-T) as displayed in the inset. It follows a square-root law for larger values of (T_c-T).

cooling near the temperature of transition (Fig. 4). These evolutions possibly are a precursor effect of the transition to the monoclinic phase and the analysis of these thermal displacement ellipsoids[16,17] provides key information about the main amplitudes involved in the eventual phonon freezing. Concerning the monoclinic phase, within a one-phonon condensation mechanism, just below the phase transition, the frozen phonon brings the main contribution to the observed atomic displacements. Indeed, in the low-temperature phase, the atomic positions should be inferred from the novel coordinates of the soft phonon. Within a mean-field approach, the thermal dependence of these displacements in the monoclinic phase should be proportional to the square root of $(T_C - T)$. Actually, the results diplayed in Figs. 5 –7present different behaviors and some displacements clearly exhibit the classical thermal evolution approching a transition while others do not exhibit any significant temperature dependence. Moreover, the observed atomic displacements displaying a temperature dependence in the monoclinic phase do not correspond (Fig. 7) to the main components of the phonon expected to soften in the tetragonal phase as we have determined by the analysis of u^{ij}.

TABLE I. Thermal-expansion coefficients fitted from our neutron-diffraction results and compared to previous works in the monoclinic and tetragonal phases. The values of thermal-expansion coefficients in the two phases are extracted from Fig. 2.

	Present work $\alpha\ [K^{-1}]$	Previous works $\alpha\ [K^{-1}]$
a_m	7.16	9.5
b_m	2.16	1.5
c_m	1.26	1.4
a_t	10.80	12.5
c_t	13.70	14.5

Therefore a more complex mechanism must be considered to explain this situation and it is extremely important to identify all the order parameters of this phase transition. Following the theoretical work by Negita,[9] based on group theory, this phase transition can be described by the condensation of two phonons belonging respectively to M_1 and M_2 irreducible representations at the M point of the tetragonal Brillouin zone $[k_M=(\pi/a_t,\pi/a_t,0)]$. Therefore it is interesting to classify these displacements in the monoclinic phase and the anisotropic thermal displacements in the tetragonal phase according to the irreducible representations M_1 and M_2. The compatibility relations between the two phases imply a well defined order for these phonon condensations: the only way to obtain the monoclinic phase is the phonon belonging to M_1 irreducible representation be the first one to freeze. This doubles the unit cell, leading to an orthorhombic phase (*Pbcn*). Since no experimental evidence exists for this phase, the second condensation (M_2) should immediately

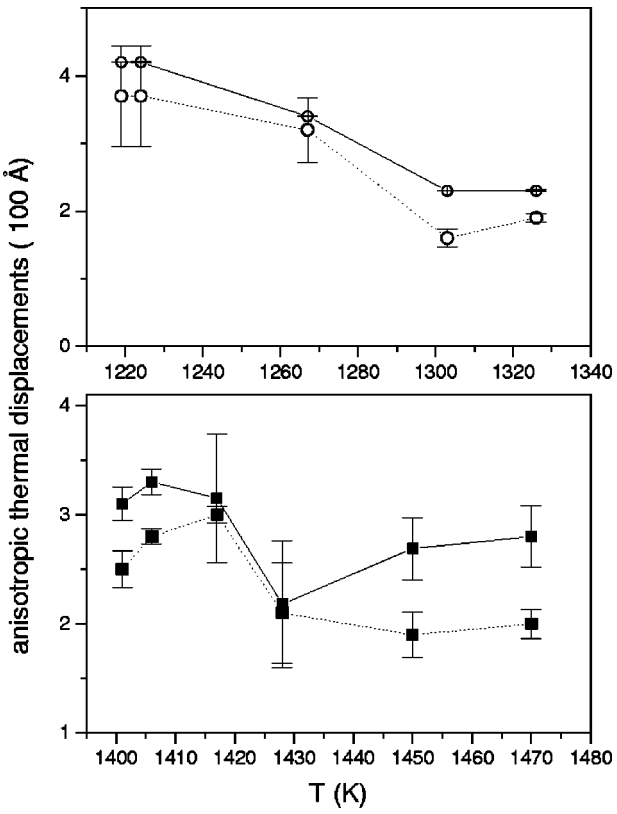

FIG. 4. Variation of the anisotropic mean-square displacements u^{11} (Zr) (dotted lines) and u^{33} (O) (solid line) in the tetragonal phase on heating (bottom panel) and on cooling (top panel). The other anisotropic thermal displacememts decrease with the temperature.

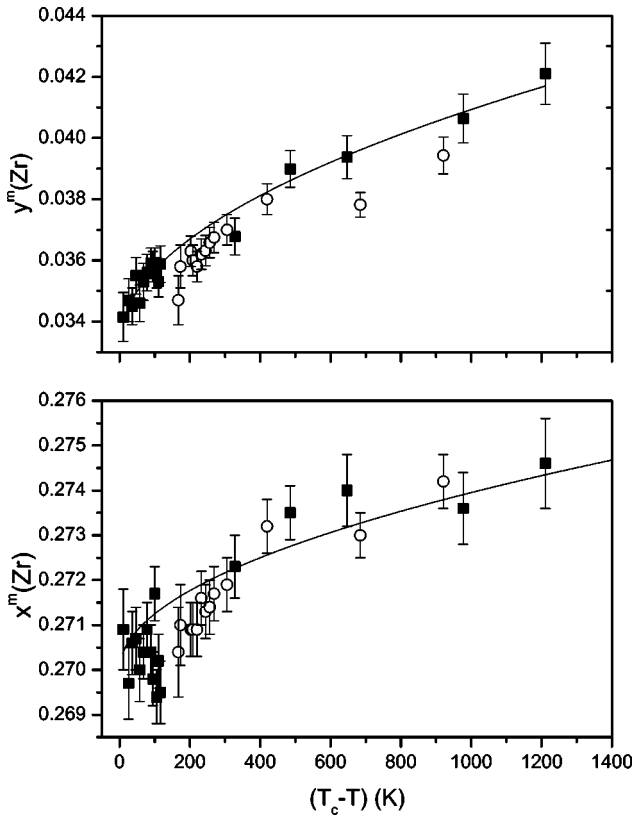

FIG. 5. Variation of the x and y fractional coordinates of Zr atoms in the monoclinic phase on heating (squares) and on cooling (open dots). The full line represents a fit with a square-root law (T_c-T). These atomic displacements are related to the M_1 irreducible representation.

follow the first one leading to the observed monoclinic phase. The symmetry adapted eigenvectors associated with the different representations are summarized in Table II.

From this analysis, the main components of the anisotropic thermal displacement parameters of Zr and O in the tetragonal phase behave according to the M_1 irreducible representation. The mean static atomic displacements of Zr and O(1) follow a square root evolution versus temperature and O(2) behaves according to the M_2 irreducible representation in the monoclinic phase (Fig. 7). Therefore these experimental results fully support the two phonon condensation mechanism for this phase transition.

The computation of zirconia phonon spectra using short-range interatomic potentials published by Mirgorodsky *et al.*[13] supports the softening of the M_2 phonon in the tetragonal phase. Unfortunately, this calculation is not able to also reproduce the softening of the M_1 phonon.

IV. DISCUSSION

Within this analysis of the thermal evolution of the structures of pure zirconia, a virtual intermediate phase must be involved. Since no experimental evidence exists for such an orthorhombic phase (*Pbcn*) induced by the condensation of the M_1 mode, this phase is expected to be unstable. This orthorhombic phase should transform into the monoclinic low-temperature one through a sudden condensation at the Γ point of this *Pbcn* phase. The compatibility relations between the three space groups are displayed in Fig. 8. To reproduce the unstable character of this intermediate phase, the Landau free energy $F(M_1,M_2)$, describing the tetragonal to monoclinic phase transition, should exhibit a critical saddle point. After the M_1 condensation, any variation of the M_2 order parameter, now a zone center mode belonging to the B_{2g} irreducible representation in the *Pbcn* phase, would be amplified, allowing large atomic displacements, and explaining the semireconstructive character of the phase transition.

The analysis of the evolution of the structures in the two phases allows a precise characterization of the primary order parameters M_1 and M_2. To take into account all the experimental observations, this analysis has to include also the possible couplings with the secondary order parameters as, for instance, the monoclinic distortion. From symmetry arguments, it is possible to find and to discuss all the possible couplings among primary and secondary order parameters. Such an analysis allows us to build an expression for the Landau free energy.

Provided the $(100)_m \parallel (110)_t$ and $[010]_m \parallel [001]_t$ orientations, the compatibility relations obtained by our analysis lead to the condensation of M_2^1 and M_2^2 phonons (Fig. 8); the corresponding primary order parameters are respectively labeled ϕ and η in the following. Using two basis invariants,

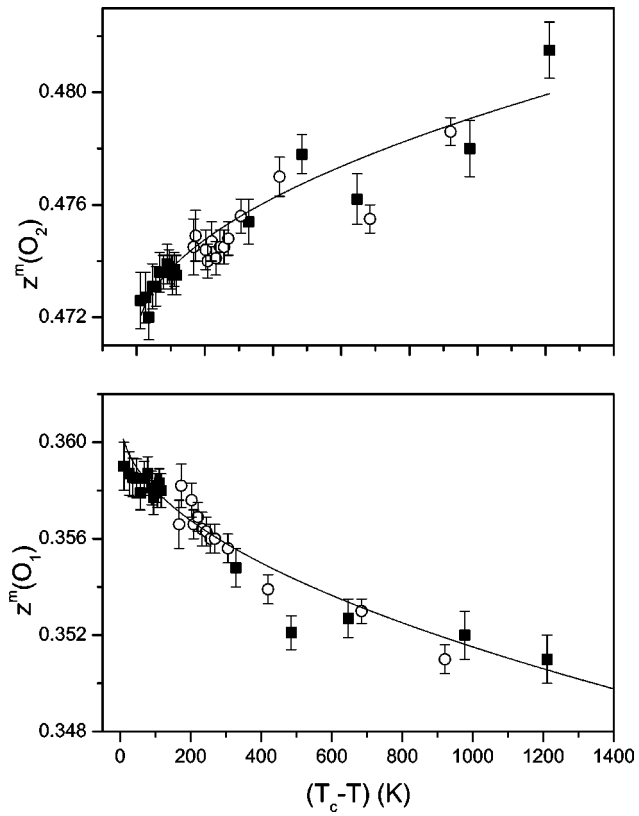

FIG. 6. Variation of the z fractional coordinate of O(1) (top panel) and of O(2) (bottom panel) versus (T_c-T) in the monoclinic phase on heating (squares) and on cooling (open dots). They exhibit a square- root dependence (full lines), and they are related to the M_1 irreducible representation.

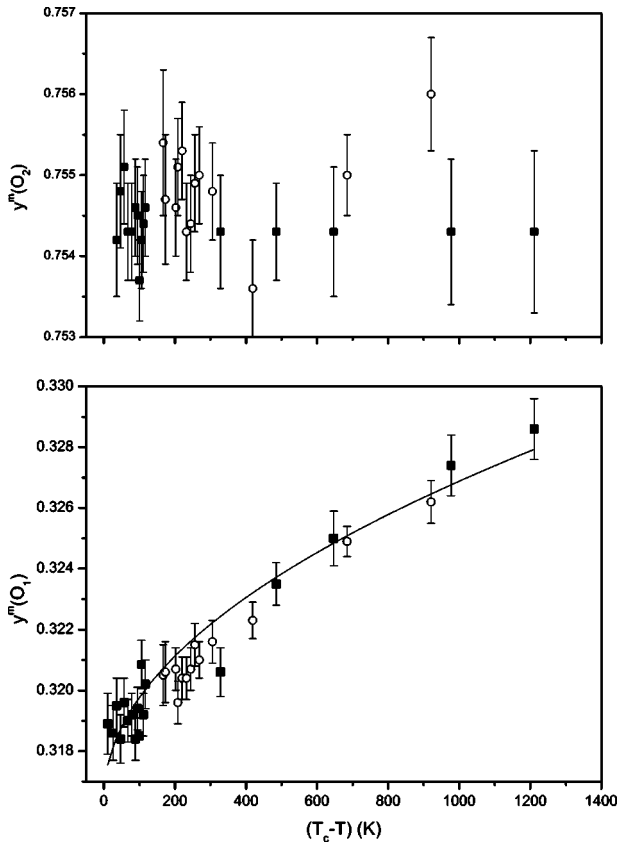

FIG. 7. Variation of the y fractional coordinate of O(1) (top panel) and of O(2) (bottom panel) versus (T_c-T) in the monoclinic phase on heating (squares) and on cooling (open dots). No clear evolution of y[O(2)] is observed whereas the behavior of y[O(1)], related to the M_2 irreducible representation, follows a square-root law.

$I_1=\eta^2+\phi^2$ and $I_2=\eta^2\phi^2$, the corresponding Landau free energy term is

$$F^1(I_1,I_2)=\frac{a}{2}I_1+\frac{b}{4}(I_1^2-2I_2)+\frac{c}{2}I_2+\frac{d}{6}(I_1^3-3I_2I_1). \tag{1}$$

This equation is expected to obey the usual conditions $a=\alpha(T-T_c)$ where α and d are positive.[22] To describe the first-order nature of the transition, this expansion should include[22] at least I_1^3. Therefore this is the simplest form of the Landau energy (cf. the Appendix) able to produce a saddle point associated with the unstable orthorhombic *Pbcn* phase.

In the tetragonal phase, there are four components of the spontaneous strain tensor allowed by symmetry: e_1+e_2 and e_3 belonging to A_{1g}, e_5 and e_6 belonging respectively to the E_g and B_{2g} irreducible representations. These terms are characterized by $\mathbf{k}=0$ and so are not involved in the doubling of the unit cell occurring at the phase transition. These strain components explain the observed large volume change associated with the phase transition and they are expected to behave like secondary order parameters. The corresponding term of the Landau free energy associated with this elastic energy is

$$F^2(e_1,e_2,e_3,e_5,e_6)=\frac{C_{11}}{2}(e_1^2+e_2^2)+\frac{C_{33}}{2}e_3^2+C_{12}e_1e_2+C_{13}(e_1e_2+e_2e_3)+\frac{C_{44}}{2}e_5^2+\frac{C_{66}}{2}e_6^2, \tag{2}$$

where C_{ij} are the isothermal elastic constants[23] and e_j is the strain field, indexed in the Voigt notation.

All the possible couplings between primary and secondary order parameters can be built looking at the decomposition onto irreducible representations of the symmetrized square of M_1+M_2. The decomposition of this representation in terms of irreducible representations of $P4_2/nmc$ is

$$[M_1+M_2]^2=2A_{1g}\oplus E_g\oplus B_{2g}\oplus A_{2u}\oplus B_{2u}\oplus E_u.$$

Therefore it can be shown that the expression of these couplings in the Landau free energy is

$$F^3=f_1(e_1+e_2)(\eta^2+\phi^2)+f_2e_3(\eta^2+\phi^2)+f_3e_6(\eta^2-\phi^2)+f_4e_5\eta\phi, \tag{3}$$

TABLE II. Symmetry adapted eigenvectors (non-normalized) at the M point of the tetragonal Brillouin zone.

		M point							
		M_1^1	M_1^2	M_2^1	M_2^2	M_3^1	M_3^2	M_4^1	M_4^2
	Δx	α	α	0	0	α	α	0	0
Zr1	Δy	α	$-\alpha$	0	0	$-\alpha$	α	0	0
	Δz	0	0	α	α	0	0	0	0
	Δx	α	$-\alpha$	0	0	α	$-\alpha$	0	0
Zr2	Δy	α	α	0	0	$-\alpha$	$-\alpha$	0	0
	Δz	0	0	α	$-\alpha$	0	0	0	0
	Δx	0	0	β	β'	0	0	δ	δ'
O1	Δy	0	0	γ	γ'	0	0	ϵ	ϵ'
	Δz	β	β	0	0	β	β	0	0
	Δx	0	0	$-\beta$	β'	0	0	δ	$-\delta'$
O2	Δy	0	0	$-\gamma$	γ'	0	0	ϵ	$-\epsilon'$
	Δz	$-\beta$	β	0	0	$-\beta$	β	0	0
	Δx	0	0	γ	$-\gamma'$	0	0	ϵ	$-\epsilon'$
O3	Δy	0	0	β	$-\beta'$	0	0	δ	$-\delta'$
	Δz	β	$-\beta$	0	0	$-\beta$	$-\beta$	0	0
	Δx	0	0	$-\gamma$	$-\gamma'$	0	0	ϵ	ϵ'
O4	Δy	0	0	$-\beta$	$-\beta'$	0	0	δ	δ'
	Δz	$-\beta$	$-\beta$	0	0	β	$-\beta$	0	0

where the f_i are phenomenological coefficients.

The total Landau free energy is the sum of the three parts F^1, F^2, and F^3 discussed above. Figure 9 presents the different extrema (i.e., the stable and the unstable phases) associated with this free energy (cf. the Appendix). The monoclinic phase lies on the first-order transition line as expected. Minimizing this free energy with respect to the strain leads to a dependence of e_5 (the distortion angle $\pi/2-\beta$) proportional to $\phi\eta$. Since both ϕ and η follow a square-root dependence on (T_c-T), the expected evolution of e_5 versus temperature is linear.

This linear evolution of e_5 is actually observed only near the phase transition (Fig. 3). On the other hand, this model gives a straightforward explanation of the square-root dependence of the monoclinic distortion $(\pi/2-\beta)$ far from the transition. It is interesting to point out that the two parameters present a different behavior versus temperature far from the phase transition since z(Zr), x(O1), and x(O2) do not display any significant variation while z(O1) and z(O2) exhibit a square-root dependence (Fig. 6). Since the atomic displacements associated to M_2 exhibit a locking 150 K below T_c [evolution of x_m(O1) in Fig. 6] while the atomic displacements associated with M_1 continue to evolve according to the square-root law, the product of the two primary order parameters (i.e., e_5) will follow a square-root law far from the phase transition as experimentally observed. This behavior seems to be related to the need to reduce the important Coulombian repulsion occurring between the anions in the ZrO(1) polyhedron.

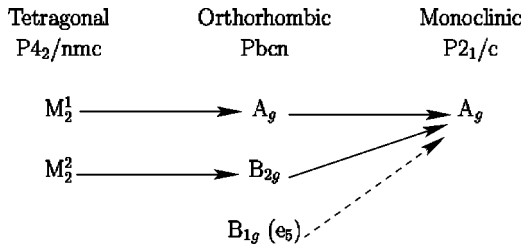

FIG. 8. Compatibility relations of the irreducible representations in the three phases describing the tetragonal to monoclinic phase transition sequence.

V. CONCLUSION

Accurate data on zirconia structures, extracted by Rietveld refinement of neutron-diffraction patterns, allow a microscopic description of the tetragonal to monoclinic first-order phase transition. Only the tetragonal and the monoclinic phases were observed in the diffraction patterns in the investigated temperature range. No intermediate phase was detected close to the transition temperature either on heating or on cooling. In the high-temperature phase (tetragonal), the anisotropic mean-square displacements of Zr and O atoms were analyzed and interpreted in terms of the softening of a mode belonging to the M_1 irreducible representation. In the low-temperature phase (monoclinic), several static atomic displacements of Zr, O(1), and O(2) atoms display a square-root evolution versus temperature, suggesting the condensation of another mode belonging to the M_2 irreducible representation. Group theory clearly confirms the order of these condensations and the symmetry of these two phonons. Thus a Landau free energy is built to describe all the possible couplings between these modes, the primary order parameters, and the strain field, the secondary order parameter, induced during the phase transition by the volume

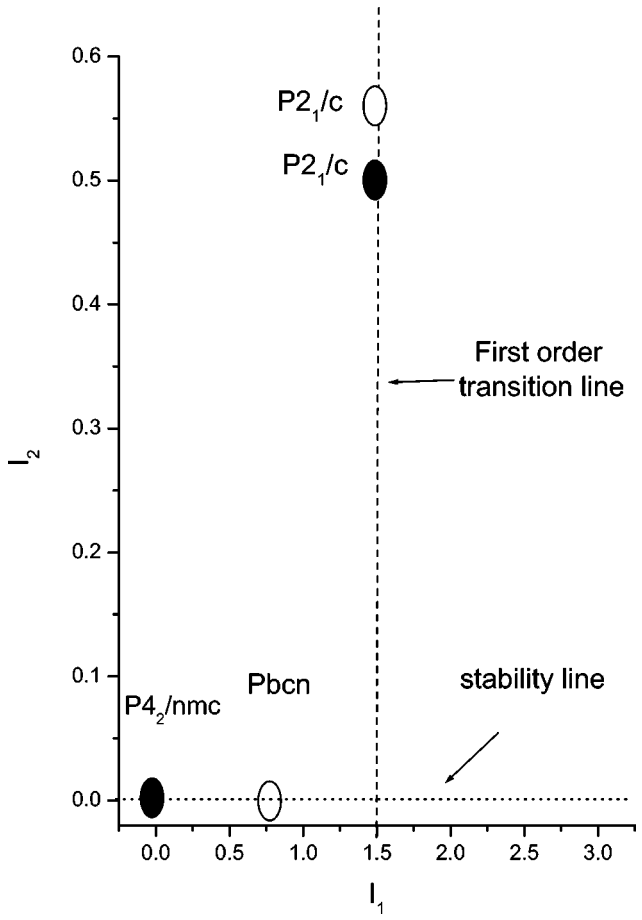

FIG. 9. Schematic description of the phase diagram in the (I_1,I_2) plane $(d=c=-a=-2b=1)$. Full dots and open dots represent stable and unstable phases, respectively. The stability line (dotted) and first-order transition line (dashed) are displayed.

difference between the two phases. This analysis predicts and explains the observed evolution of the monoclinic distortion versus temperature.

Within this framework, the first-order semireconstructive tetragonal to monoclinic phase transition is described as a two stage process. The condensation of the M_1 phonon in the tetragonal phase ϕ produces an orthorhombic phase (*Pbcn*) (Fig. 9). This phase is never observed experimentally because it is unstable and associated with a critical saddle point of the Landau free energy. Therefore any instability related to the condensation of the second phonon belonging to M_2 irreducible representation η at this saddle point is amplified. This leads to the actual monoclinic phase, characterized by a drastic change in the Zr coordination. This semireconstructive character of the phase transition explains the observed strain and volume change.

Such a description of the tetragonal to monoclinic phase transition helps to explain the behavior of pure zirconia under irradiation.[24] Pure monoclinic zirconia becomes tetragonal when irradiated by charged ions at room temperature. The structure of this tetragonal phase is strongly perturbed by the ballistic collisions[25,26] occurring during the irradiation process. The radiation damage heavily affects the zirconium and oxygen sublattices preventing the M_1 phonon condensation. A thermal annealing at 573 K of the irradiated samples[2] restores the monoclinic $P2_1/c$ phase and so the usual phase-transition sequence.

The mechanism presented in this paper may also explain the stability of the nanometric particles of tetragonal zirconia[27,28] at room temperature. In this case, the energy contribution related to the surface effects may produce a renormalization of the transition temperature calculated with the Landau free-energy expansion.

Finally, the unstable intermediate orthorhombic phase occurring in this phase transition can also be useful to understand the complex pressure-temperature phase diagram of pure zirconia where different orthorhombic phases appear at high pressure.[1]

APPENDIX: LANDAU FREE ENERGY

The total Landau free energy F describing the phase transition is the sum of three terms: F^1, a term induced by atoms displacements [Eq. (1)]; F^2, an elastic energy term [Eq. (2)]; and a coupling term F^3 [Eq. (3)]. The equilibrium condition for the low-symmetry phase leads to the minimization of $F=F^1+F^2+F^3$ with respect to the strain field. This leads to the following relation between first-order parameters and the second-order parameter e_5:

$$\sin\left(\frac{\pi}{2}-\beta\right)\alpha e_5=-\frac{f_4\phi\eta}{C_{44}}. \tag{A1}$$

This equation clearly shows that e_5 exhibits a linear behavior versus temperature if we suppose that C_{44} does not vary significantly with the temperature. This result agrees with experimental data (linear part of Fig. 3).

Using the equilibrium conditions, it is possible to rewrite F only as a function of the invariant basis set. F, the total Landau free energy, is then described by Eq. (1) with new values of the phenomenological coefficients now depending on the different isothermal elastic constants of the tetragonal phase,

$$F(I_1,I_2)=\frac{a}{2}I_1+\frac{b}{4}(I_1^2-2I_2)+\frac{c}{2}I_2+\frac{d}{6}(I_1^3-3I_2I_1). \tag{A2}$$

The minimization of F leads to four solutions: the trivial one corresponding to the tetragonal phase,

$$(I_1,I_2)=(0,0), \tag{A3}$$

two possible monoclinic phases with nontrivial invariant values,

$$(I_1,I_2)=\left(\frac{c-b}{d},\frac{ad+c^2-bc}{d^2}\right), \tag{A4}$$

$$(I_1,I_2)=\left(\frac{-b+\sqrt{b^2-2(2a+c)d}}{2d},\frac{-b+\sqrt{b^2-2(2a+c)d}}{16d^2}\right). \tag{A5}$$

The stable monoclinic phase is described by the solution (A5). The fourth solution corresponds to a phase with a trivial invariant value,

$$(I_1, I_2) = \left(\frac{-b + \sqrt{b^2 - 4ad}}{2d}, 0 \right), \tag{A6}$$

and it can be identified with an orthorhombic phase ($\phi \neq 0, \eta = 0$).

The different transition temperature associated to the first-- order phase transition are equal to

$$T_1 = T_c - \frac{16dc - 3b^2}{32d\alpha}, \quad T_2 = T_c - \frac{2cd - b^2}{4d\alpha}. \tag{A7}$$

Taking into account the existence of these four phases and the stability condition for the existence of the monoclinic phase, we obtain a set of inequalities for the phenomenological coefficients which allow us to describe a part of the phase diagram in the (I_1, I_2) plane (cf. Fig. 9).

[1] E. Kisi and C. Howard, Key Eng. Mater. **153–154**, 1 (1998).
[2] D. Simeone, D. Gosset, J.L. Bechade, and A. Chevarier, J. Nucl. Mater. **300**, 27 (2002).
[3] J. Katamura and T. Sakuma, Acta Mater. **46**, 1569 (1998).
[4] P. Schelling, S. Phillpot, and D. Wolf, J. Am. Ceram. Soc. **84**, 1609 (2001).
[5] E. Subbarao, H. Maiti, and K. Srivastava, Phys. Status Solidi A **21**, 9 (1974).
[6] R. Patil and E. Subbarao, Acta Crystallogr., Sect. A: Cryst. Phys., Diffr., Theor. Gen. Crystallogr. **26**, 535 (1970).
[7] T. Mitssuhashi, Y. Fujiki, M. Tsukokia, and N. Tsuda, J. Phys. Soc. Jpn. **30**, 1206 (1971).
[8] A. Hueur and M. Ruhle, Acta Metall. **12**, 2101 (1985).
[9] K. Negita and H. Takao, J. Phys. Chem. Solids **50**, 1325 (1989).
[10] D. Argyriou and M. Elcombe, J. Phys. Chem. Solids **57**, 343 (1996).
[11] A. Mirgorodsky, M. Smirnov, P. Quintard, and T. Merle Mejean, Phys. Rev. B **52**, 9111 (1995).
[12] A. Mirgorodsky, M. Smirnov, and P. Quintard, Phys. Rev. B **55**, 19 (1997).
[13] A. Mirgorodsky, M. Smirnov, and P. Quintard, J. Phys. Chem. Solids **60**, 985 (1999).
[14] G. Rignanese, F. Detraux, X. Gonze, and A. Pasquarello, Phys. Rev. B **64**, 134301 (2001).
[15] X. Zhao and D. Vanderbilt, Phys. Rev. B **65**, 075105 (2002).
[16] F. Frey, H. Boysen, and T. Vogt, Acta Crystallogr., Sect. B: Struct. Sci. **46**, 724 (1990).
[17] H. Boysen, F. Frey, and T. Vogt, Acta Crystallogr., Sect. B: Struct. Sci. **47**, 881 (1991).
[18] J.F. Bérar, *Accuracy in Powder Diffraction II, Proceedings of the International Conference*, NIST special publication (1992), Vol. 846, p. 212.
[19] G. Wolten, Acta Crystallogr. **17**, 763 (1964).
[20] S. Lang, J. Am. Ceram. Soc. **47**, 641 (1964).
[21] J.C. Toledano and P. Toledano, *Landau Theory of Phase Transitions* (World Scientific, Singapore, 1987), Chap. 4.
[22] P. Toledano and V. Dimitriev, *Reconstructive Phase Transition* (World Scientific, Singapore, 1996).
[23] R. Cohen, M. Mehl, and L. Boyer, Physica B **150**, 1 (1988).
[24] D. Simeone, X. Deschanel, D. Gosset, J.P. Bonal, and E. Berthoumieux, J. Nucl. Mater. **297**, 244 (2001).
[25] G. Martin, Phys. Rev. B **30**, 1424 (1984).
[26] P. Bellon and G. Martin, Phys. Rev. B **39**, 2403 (1989).
[27] R. Garvie, J. Phys. Chem. **82**, 218 (1978).
[28] P. Bouvier and G. Lucazeau, J. Phys. Chem. **61**, 569 (2000).